Atmos. Chem. Phys., 11, 7133–7142, 2011
www.atmos-chem-phys.net/11/7133/2011/
doi:10.5194/acp-11-7133-2011

Atmospheric Chemistry and Physics

Ab initio studies of $O_2^-(H_2O)_n$ and $O_3^-(H_2O)_n$ anionic molecular clusters, $n \leq 12$

N. Bork[1], T. Kurtén[2,3], M. B. Enghoff[1], J. O. P. Pedersen[1], K. V. Mikkelsen[2], and H. Svensmark[1]

[1]National Space Institute, Technical University of Denmark, Juliane Maries Vej 30, 2100 Copenhagen Ø, Denmark
[2]Department of Chemistry, H.C. Ørsted Institute, University of Copenhagen, Universitetsparken 5, 2100 Copenhagen Ø, Denmark
[3]Division of Atmospheric Sciences and Geophysics, Dept. of Physics, P.O. Box 64, 00014 University of Helsinki, Finland

Received: 17 March 2011 – Published in Atmos. Chem. Phys. Discuss.: 6 May 2011
Revised: 12 July 2011 – Accepted: 13 July 2011 – Published: 21 July 2011

Abstract. An ab initio study of gaseous clusters of O_2^- and O_3^- with water is presented. Based on thorough scans of configurational space, we determine the thermodynamics of cluster growth. The results are in good agreement with benchmark computational methods and existing experimental data. We find that anionic $O_2^-(H_2O)_n$ and $O_3^-(H_2O)_n$ clusters are thermally stabilized at typical atmospheric conditions for at least $n = 5$. The first 4 water molecules are strongly bound to the anion due to delocalization of the excess charge while stabilization of more than 4 H_2O is due to normal hydrogen bonding. Although clustering up to 12 H_2O, we find that the O_2 and O_3 anions retain at least ca. 80 % of the charge and are located at the surface of the cluster. The O_2^- and O_3^- speicies are thus accessible for further reactions. We consider the distributions of cluster sizes as function of altitude before finally, the thermodynamics of a few relevant cluster reactions are considered.

1 Introduction

Understanding the properties of clouds is one of the most challenging and important subjects within atmospheric chemistry. Recently, several studies have suggested that cloud formation is correlated to the influx of cosmic rays and that cosmic rays may contribute to the production of especially low clouds (Marsh and Svensmark, 2000; Carslaw et al., 2002; Enghoff et al., 2008; Svensmark et al., 2009). The primary effect of cosmic rays is ionization of the atmosphere, producing a variety of molecular cations and free electrons. It has therefore been speculated that the cloud forming effect of cosmic rays is arising from the ions produced. This mechanism seems plausible since both the physical and chemical properties of ions are so different from those of uncharged species. See for example reviews by Harrison and Carslaw (2003) and Enghoff and Svensmark (2008).

A free electron is very reactive and will most likely be accepted by an O_2 or O_3 due to the abundance and electron affinity of O_2 and O_3. It is well known that small ions have a high affinity for water and that such ions quickly become hydrated under usual atmospheric conditions. The most important atmospheric hydration mechanism is the stepwise condensation of one H_2O to the cluster,

$$O_2^-(H_2O)_{n-1} + H_2O \rightarrow O_2^-(H_2O)_n \quad \text{(R1)}$$

$$O_3^-(H_2O)_{n-1} + H_2O \rightarrow O_3^-(H_2O)_n. \quad \text{(R2)}$$

Both charge transfer and oxidation of a third species are then possible. Another likely event is reaction with a cation.

For studying these reactions, knowledge of the structures of the most populated $O_2^-(H_2O)_n$ and $O_3^-(H_2O)_n$ clusters is fundamental since any subsequent reactions may be dependent upon the degree of solvation (Kurtén et al., 2007; Bandy and Ianni, 1998; Gross et al., 2008; Nadykto et al., 2006, 2008). Currently, the distribution of the most stable and most important clusters remains uncertain and hence the geometries, thermodynamics, and electronic properties are all unknown.

From both theory and experiment it is known that Reactions (R1) and (R2) are highly exothermic for small n.

Correspondence to: N. Bork
(nbor@space.dtu.dk)

It is however inevitable that the thermodynamics will converge towards that of ordinary hydrated water for large n ($\Delta G^\circ_{298K} = -8.6$ kJ/mol) (Lide, 1997). This convergence has not yet been demonstrated and is of interest for studying solvated ions in general.

A number of studies of both $O_2^-(H_2O)_n$ and $O_3^-(H_2O)_n$ clusters have previously been published. Experimental studies in the 1970's determined the thermodynamics of cluster growth for both O_2^- and O_3^-, although only including up to 3 H_2O (Arshadi and Kebarle, 1970; Fehsenfeld and Ferguson, 1974). More recently, large metastable $O_2^-(H_2O)_n$ and $O_2^-(H_2O)_n$ clusters have been produced via negative corona discharges. Confirmed by several studies, clusters containg between 3–15 H_2O is readily produced despite very different experimental conditions (Yang and Castleman, 1990; Skalny et al., 2008; Hvelplund et al., 2010). Also recently, the thermodynamics of 1–5 H_2O clusters has been studied using ab initio methods (Seta et al., 2003; Lee and Kim, 2002). Although in qualitative agreement with the experimental data, the difference is on the order of 5–10 kJ/mol.

To solve these issues we have undertaken an ab initio study of the initial clustering reactions of O_2^- and O_3^- with water, i.e. Reactions (R1) and (R2), to firmly establish the sizes and properties of these. We have included up to 12 H_2O which constitute at least two hydration shells. Based on thorough scans of configurational space, we present thermodynamics of Reactions (R1) and (R2) and analyse the resulting structures. Further, we analyse the charge distributions of the clusters and determine the reactivity towards some relevant reactions.

2 Computational details

Due to the sizes of the clusters combined with the vast amount of possible configurations, optimization of the computational procedure was important. Initially, all structures were optimized using Hartree-Fock theory (HF). Subsequently, the most promising candidates were optimized using density functional theory (DFT).

The anionic charge of the clusters is a known challenge to DFT (Jensen, 2010). Addressing this problem, we utilized the Coulomb-attenuating method via the CAM-B3LYP functional (Yanai et al., 2004). This newly developed functional is based on the well known B3LYP functional, but is incorporating an increasing amount of exact HF exchange at increasing distances. By this, the CAM-B3LYP functional is optimized towards studying charged systems and results are generally much improved compared to standard B3LYP results (Peach et al., 2006; Yanai et al., 2004).

Also concerning the basis set, the negative charge of the clusters is known to require special attention by inclusion of diffuse, long-range functions on all atoms (Jensen, 2010; Kurtén et al., 2008). We utilised the Dunning style basis set aug-cc-pVDZ (Dunning, 1989) since this basis set is small enough to allow calculations on the clusters of interest but large enough to produce accurate results (Seta et al., 2003). However, for scanning configurations at the HF level, the smaller cc-pVDZ basis set was used.

All HF and DFT calculations were performed using the Gaussian 09 package (http://gaussian.com/). Standard convergence criteria were employed.

To confirm the energetics of the CAM-B3LYP calculations, single point calculations using explicitly correlated coupled cluster theory CCSD(T)-F12a (Adler et al., 2007) with the VDZ-F12 basis set (Peterson et al., 2008) were performed. These calculations were performed using the MOLPRO 2010.1 package (http://molpro.net/). The explicitly correlated calculations used density fitting (Manby, 2003; Werner et al., 2007) and resolution of the identity approximations with the default auxiliary basis sets (Weigend, 2002; Weigend et al., 2002; Yousaf and Peterson, 2008). Test calculations on the $O_2^-(H_2O)_1$ cluster indicate that the difference between VDZ-F12 and VTZ-F12 binding energies is less than 0.5 kJ/mol.

The CCSD(T)-F12 calculations are based on a restricted open-shell Hartree-Fock reference. Both restricted-open shell and unrestricted coupled-cluster calculations were performed; the difference between these was less than 4 kJ/mol in all cases. Values of the T1 and D1 diagnostics ranged between 0.011–0.039 and 0.03–0.24, respectively. This indicates that some of the studied systems (mainly the $O_2^-(H_2O)_1$ cluster, and all the $O_3^-(H_2O)_n$ clusters) have partial multireference character. However, the CCSD(T)-F12a results are still expected to be at least qualitatively reliable.

Since only including up to 5 H_2O, previous ab initio studies of $O_2^-(H_2O)_n$ and $O_3^-(H_2O)_n$ clusters have not applied systematic scans of configurational space. In the present study the high number of solvent water molecules induce countless possible configurations and thus require a fully systematic approach. Here, we have utilized the simulated annealing method (SA) (Corana et al., 1987) implemented via the Born-Oppenheimer molecular dynamics technique (Li et al., 2000). The main advantage of SA is that the algorithm is not just able to determine the nearest local minima, but also able to migrate from minima to minima. However, even considering mid-sized clusters it is practically impossible to scan all configurations. We chose to terminate the procedure when the same minimum had been confirmed by at least 3 independent calculations for the mid sized clusters (1–7 H_2O) and 2 independent calculations for the 8–10 H_2O clusters. For the 11 and 12 H_2O clusters, the procedure was terminated after 25 SA runs despite no confirmed minimum. Therefore, for clusters containing more than 8 H_2O but especially for 11 and 12 H_2O clusters, the probability of undiscovered but more stable configurations is non-negligible.

The optimization were as follows: Initially, a number of randomly generated structures (between 5 and 15) were relaxed at the HF/cc-pVDZ level of theory and used as input for

Table 1. Entropy and Gibbs free energy of Reactions (R1) and (R2) at standard conditions ($T = 298.15$ K, $p = 1$ bar). Units are J/mol·K and kJ/mol. The values of ΔG are plotted in Fig. 1 as function of n.

	Reaction (R1)		Reaction (R2)	
n	ΔS	ΔG	ΔS	ΔG
1	−102.3	−61.5	−99.4	−48.5
2	−115.3	−42.6	−133.2	−23.5
3	−130.9	−26.8	−121.4	−17.5
4	−129.8	−21.1	−135.9	−19.2
5	−131.8	−19.5	−171.5	−17.9
6	−169.5	−2.6	−110.9	−10.7
7	−124.7	−6.3	−171.2	−10.7
8	−146.6	−24.2	−147.9	−15.6
9	−149.8	−9.7	−134.6	−12.1
10	−138.0	−5.7	−154.5	−9.6
11	−140.6	−5.3	−138.9	−10.7
12	−115.0	−13.4	−90.3	−6.2

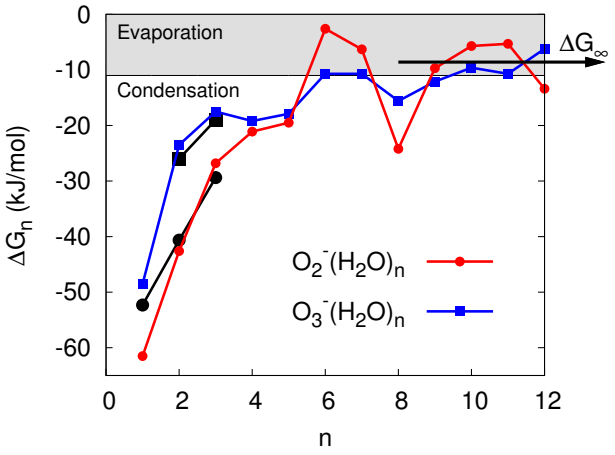

Fig. 1. ΔG for Reactions (R1) and (R2). Regimes implying condensation and evaporation are indicated for 298 K and 50 % relative humidity. ΔG_∞ denotes the value of hydrated H_2O. Black spheres and squares are experimental data from Arshadi and Kebarle (1970) and Fehsenfeld and Ferguson (1974), respectively.

the SA procedure. Complimentary to these, also structures based on adding one H_2O to the previous cluster were considered. The structures were thereafter given 10–50 kJ/mol of kinetic energy per H_2O which was uniformly removed during a time period of ca. 500 femtoseconds. The SA algorithm weight the vibrational frequencies as

$$w_i = \left[1 + \exp\left(-\beta(E_F - \omega_i)\right)\right]^{-1/2} \quad (1)$$

where ω_i is the i'th vibrational mode and E_F if the Fermi energy parameter. Using a Fermi-Dirac inverse temperature $\beta > 0$, all frequencies above E_F hereby are repressed while all frequencies below E_F are enhanced (Santos et al., 2009). We chose $E_F = 700\ \mathrm{cm}^{-1}$ and $\beta = 0.1$ cm, since these values will effectively repress intermolecular vibrations while enhancing modes corresponding to molecular translation.

After termination of the SA procedure, the 5–10 most stable structures were re-relaxed using CAM-B3LYP/aug-cc-pVDZ. In no cases were major discrepancies between then most stable HF structure and the most stable DFT structure found.

For evaluating the electrochemical properties of the $O_2^-(H_2O)_n$ and $O_3^-(H_2O)_n$ clusters, knowledge of the distribution of the excess electron is important. The analysis was performed using the charge partitioning method by Bader, also known as the Atoms-In-Molecules approach (Bader, 1998, 1990). This method is especially well suited in applications with electronic structure calculations since the required input is the electronic density and nuclear coordinates. The Bader method is based on partitioning the system into atomic regions separated by zero flux surfaces, i.e. surfaces consisting of stationary points with respect to the electronic density. The method, although computationally demanding, is rigid and has been demonstrated to work well, both for charged systems (Bork et al., 2011) and water containing systems (Henkelman et al., 2006). The algorithm by Henkelman et al. was applied (Henkelman et al., 2006; Tang et al., 2009).[1]

Since atomic charge is an ill defined property, charge assignation may be ambiguous. We are however interested in the total charge of the O_2 and O_3 species and since the electronic density of the boundaries between the molecules is small compared to the total electronic density, the method is in this case unambiguous (Cochran, 1961).

3 Results and discussion

3.1 Thermodynamics

The thermodynamic data of the most stable configurations are summarized in Table 1 and illustrated in Fig. 1.

First, we note that the O_2^- anion is significantly more water affinitive than the O_3^- anion for $n \leq 3$. This is likely a consequence of the size of the ions. O_3^- has three atoms to distribute the charge amongst while O_2^- has just two. Consequently, the addition of one H_2O to O_2^- yields a correspondingly larger decrease of electrostatic energy. However, uptake of the first few H_2O is significantly exothermic and will occur at all relevant atmospheric conditions for both systems.

Adding more H_2O, the reactions become smoothly less exothermic. At ca. 6–7 H_2O, the Gibbs free energy become close to that of hydrated water, $\Delta G_\infty = -8.6$ kJ/mol, but addition of the 8'th H_2O yield a strong stabilization. At even larger clusters the thermodynamics seems to fluctuate around the value of hydrated water within ca. 5 kJ/mol.

[1] Freely available from http://theory.cm.utexas.edu/bader/

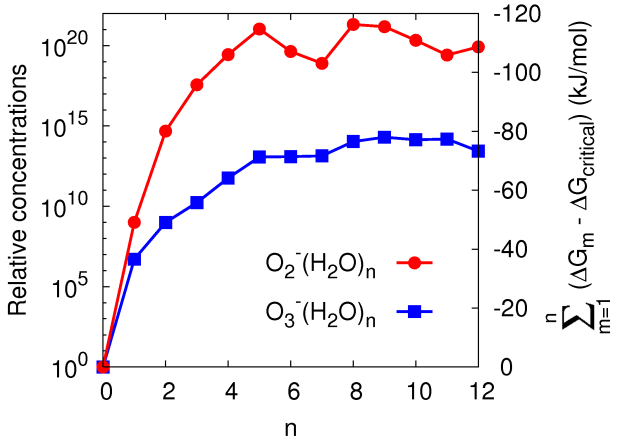

Fig. 2. Development of concentrations and accumulated energies of the $O_x^-(H_2O)_n$ clusters at 298 K and 50 % relative humidity. Both curves correspond to both vertical axis via Eq. (2).

Assuming thermal equilibrium, the law of mass action yields

$$\frac{[O_2^-(H_2O)_n]}{[O_2^-(H_2O)_{n-1}]} = [H_2O] \times \exp\left(-\frac{\Delta G}{RT}\right), \quad (2)$$

where ΔG is the Gibbs free energy change, T is the absolute temperature and R is the gas constant. Activities are here approximated by partial pressures. Equation (2) is for Reaction (R1) but equivalent for Reaction (R2). Assuming a temperature of 298 K and a relative humidity of 50 %, i.e. $p(H_2O)$ = 16 mbar, yields that $\Delta G < -10.3$ kJ/mol favor condensation, while $\Delta G > -10.3$ kJ/mol favor evaporation. This value is denoted $\Delta G_{critical}$ and is illustrated in Fig. 1, separating the evaporation and condensation regimes.

Based on Eq. (2), the concentrations of the investigated clusters were examined. Here, thermal equilibrium is assumed and possible sinks are neglected. The results are shown in Fig. 2. Note the logarithmic scale. For simplicity, the concentrations of the un-hydrated O_2^- and O_3^- ions are set to 1 and all other concentrations evaluated relative to these. Hence, the relative concentrations of the O_2^- based and O_3^- based clusters are here not directly comparable. Although the predicted concentrations are sensitive to temperature and humidity, is is clear that under these conditions clusters of multiple sizes will co-exsist. In stead, many clusters containing more than 5 H_2O may be found in significant concentrations and these clusters should all be thoroughly considered when assessing the further reactivity of these ions. For an analysis of the cluster size distributions as function of altitude, see Sect. 3.4.

Also shown in Fig. 2, on the secondary ordinate, are the accumulated stabilities relative to $\Delta G_{critical}$. These again demonstrate the absence of clusters of particular high stability. Note that the two ordinates are 1:1 linked through Eq. (2).

Table 2. Free energy differences of Reactions (R1) and (R2) from various methods. "CCSD(T)" refers to UCCSD(T)-F12/VDZ-F12 calculations on CAM-B3LYP structures. Units are kJ/mol. $*$ and $**$ indicate data from Arshadi and Kebarle (1970) and Fehsenfeld and Ferguson (1974) respectively.

Reaction (R1)		
n	ΔE(CCSD(T) − DFT)	ΔG(Exp. − DFT)
1	3.02	9.2*
2	1.50	2.0*
3	1.36	−2.5*
4	1.41	
5	−1.19	
Reaction (R2)		
n	ΔE(CCSD(T) − DFT)	ΔG(Exp. − DFT)
1	0.15	
2	0.58	2.5**
3	1.08	1.5**
4	−0.24	
5	4.52	

Experimental data up to $n = 3$ have been produced, based on mass spectrometry (Arshadi and Kebarle, 1970) and the flowing afterglow technique (Fehsenfeld and Ferguson, 1974). These results are also shown in Fig. 1 and Table 2. The comparison with the experimental result for the $O_2^-(H_2O)$ system is quite poor, differing almost 10 kJ/mol, but the remaining results are in very good agreement with experiment, within 2.5 kJ/mol. Further, the results smoothly converge towards the correct value of hydrated water and hence, both ends of the data series are confirmed. Finally, the absence of "magic numbers", i.e. clusters of particular high stability, is in accordance with the findings of Yang and Castleman (1990) and Skalny et al. (2008). In general, the agreement between these results and previous experimental data is very satisfactory.

Although the CAM-B3LYP functional has been shown to perform well on charged systems both here and previously, DFT is arguably not the ideal method for studying charged systems due to problems with charge delocalization. We therefore confirmed the relative free energies of the smallest clusters using explicitly correlated UCCSD(T)-F12/VDZ-F12 calculations. Due to computational expense, no further structural optimizations were performed and neither was entropy determined. The resulting energies are thus a measure of the ability of CAM-B3LYP to describe the electronic energies of these systems. The resulting energy differences are shown in Table 2.

The agreement between these methods of calculations is in general surprisingly good, with an average deviation of just 1.4 kJ/mol. The largest deviations are found for the $O_2^-(H_2O)$ and $O_3^-(H_2O)_5$ cluster. We note that the CAM-B3LYP results presented here are in relatively poor agreement

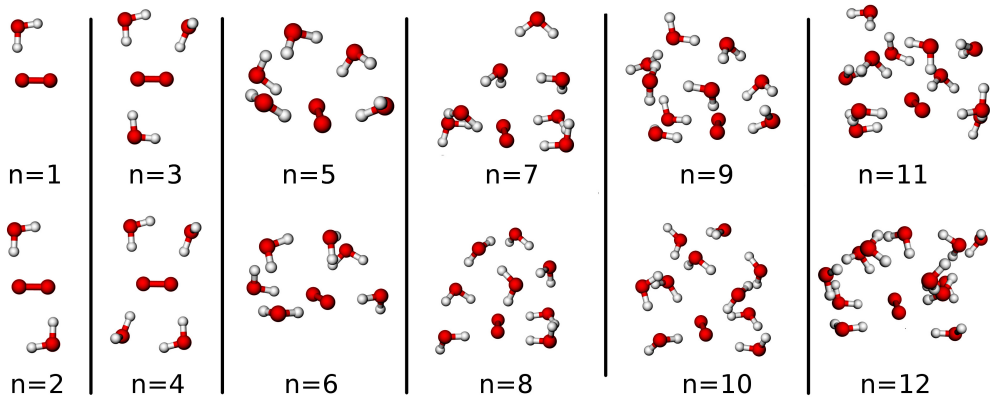

Fig. 3. Structures of the most stable $O_2^-(H_2O)_n$ clusters, $n = 1-12$. The O_2^- ions are always found inside, but near the surface of the clusters. The solvent water adopts a clear shell-like structure, shown in Fig. 5. The charge on the central ion is partially delocalized, converging at ca. 0.80 e. See also Fig. 6.

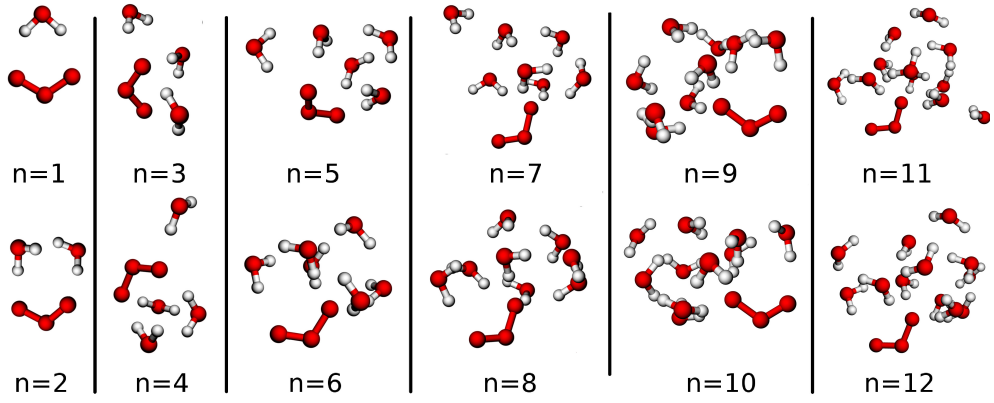

Fig. 4. Structures of the most stable $O_3^-(H_2O)_n$ clusters, $n = 1$–12. The O_3^- ions are found near the surface of the clusters, but outside the hydrogen bonded network. The solvent water adopt a clear shell-like structure, shown in Fig. 5. The charge on the central ion is partially delocalized, converging at ca. 0.82 e. See also Fig. 6.

with experiment for the $O_2^-(H_2O)$ system as well, but otherwise, no apparent reason for the increased deviation for these particular systems was found. The remaining systems all deviate less than 1.5 kJ/mol, and especially for the $O_3^-(H_2O)_n$ series, the agreement is excellent. We thus conclude that the obtained results consistently compare well with both experimental and benchmark ab initio data. This is a strong argument in favor of their general quality.

3.2 Structures

All structures are illustrated in Figs. 3 and 4.

The $O_2^-(H_2O)_n$, $n \leq 5$, structures have previously been described e.g. by Lee and Kim (2002) and Seta et al. (2003) relying on B3LYP and MP2 calculations with diffuse, double zeta basis sets. No fundamental discrepancies between these previously published structures and the structures presented here could be determined visually.

All $O_2^-(H_2O)_n$, $n \geq 4$ structures adopt a similar configuration around the O_2^- anion where 4 water molecules coordinate to the π^* molecular orbital. This is the HOMO orbital facilitating the extra electron (Weber et al., 2000). In the $n = 5$ and $n = 6$ structures, this otherwise planar configuration is bent to coordinate the remaining water. For $n \geq 7$, the structures become increasingly difficult to describe as many 3, 4 and 5 membered rings are present but the basic $n = 4$ structure is conserved.

Similar to Eq. (2) we determine the relative populations of two configurations, A and B, by

$$\frac{[A]}{[B]} = \exp\left(-\frac{\Delta G}{RT}\right). \quad (3)$$

Since we found many structures separated by less than 5–10 kJ/mol we conclude that several structures, other than the configurational ground state, are found at normal atmospheric conditions.

From the structures obtained here, illustrated in Fig. 3, it is evident that the O_2^- ion does not becomes fully hydrated for $n \leq 12$. The O_2^- species remains located inside the cluster but always at or near the surface. The accessibility of the O_2^- species is important for the reactivity of the cluster, e.g. towards charge transfer to O_3.

Although the structures are given in Fig. 3, more information regarding the hydrogen bonded network can be extracted using radial distribution functions. Here, the centre-of-mass distances of O_2^- and H_2O have been determined and are shown in Fig. 5 as function of n.

Immediately, a clear shell structure is seen. For $n \geq 6$, 5 H_2O are forming a stable first hydration shell, distanced ca. 3 Å from the central O_2^- ion. These consist of the 4 H_2O described in the previous paragraph, coordinated to the π^* orbital of the O_2^- species, and a 5'th H_2O which is positioned above these H_2O. The second hydration shell is found at distances greater than ca. 4 Å and is not fully formed at $n = 12$. From Figs. 3 and 5, it is evident that growth of the $O_2^-(H_2O)_n$ cluster is mainly by adding H_2O to the existing structure with minor rearrangement of the existing network of hydrogen bonds.

The $O_3^-(H_2O)_n$ structures have previously been described by Seta et al. (2003) for $n \leq 4$ and by Ryabinkin and Novakovskaya (2004) for $n = 5$. The structures found here are illustrated in Fig. 4. No major discrepancies were found, but generally, the structures are less ordered than the corresponding $O_2^-(H_2O)_n$ structures and visual comparison is difficult. Similar to the $O_2^-(H_2O)_n$ structures, the $O_3^-(H_2O)_n$ structures are characterized by numerous 3, 4 and 5 membered rings and again several almost iso-energetic configurations were found.

Contrary to the O_2^- systems, we note that the O_3^- species is located almost outside the cluster and thus very little shielded by the clustering H_2O towards external reactants. Also contrary to the $O_2^-(H_2O)_n$ system, no first hydration shell could visually be identified. However, studying the radial distribution functions, illustrated in Fig. 5, clear shell structure was seen. The first hydration shell is found at distances between ca. 3–4 Å containing 5 H_2O. The second shell is found between 4.5 and 5 Å containing up to 4 H_2O. A third shell seems to begin around ca. 7 Å.

In the $O_3^-(H_2O)_n$ system, the shells are further from the central ion than in the $O_2^-(H_2O)_n$ system. This is a consequence of both the size of the ion and the electronic structure. Since bond strength (Fig. 1) and bond length generally are proportional, it is not surprising that the $O_2^-(H_2O)_n$ system is more tightly bound. It is also noteworthy that for both Reactions (R1) and (R2), $\Delta G_n \ll \Delta G_{\text{critical}}$ for all $n \leq 5$, signifying the importance of completing the first solvation shell. Further cluster growth, i.e. adding to the second hydration shells, is associated with significantly less energy gain.

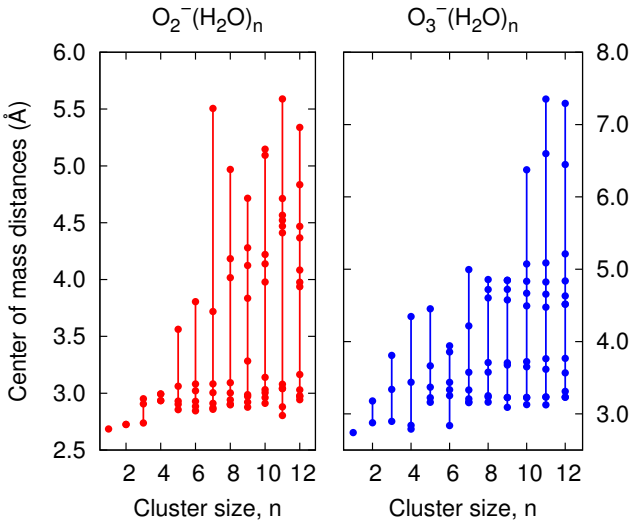

Fig. 5. Plots of center-of-mass, radial distribution functions, as function of n. In both clusters, at least two hydration shells are apparent. A complete first hydration shell contains 5 H_2O. Note the difference in scales indicating smaller and hence more stable $O_2^-(H_2O)_n$ than corresponding $O_3^-(H_2O)_n$ clusters.

3.3 Charge analysis

Studies on electrically neutral clusters of $O_2(H_2O)_n$ and $O_3(H_2O)_n$ have been published reporting binding energies much too low for clustering under atmospheric conditions (Tachikawa and Abe, 2005; Loboda and Goncharuk, 2009). It is therefore clear that the strong binding energies for the corresponding charged clusters is a direct consequence of the extra electron. Although formally located at the O_2 and O_3 species, some electronic delocalization occurs and the charge on the O_2 and O_3 species become less negative.

We have used the Bader charge partitioning method, briefly described in the "Computational details" section, to analyse the most stable clusters. The Bader charges on the O_2^- and O_3^- molecules at varying degrees of hydration are illustrated in Fig. 6.

For $n \leq 4$, each added H_2O is actively participating in dispersing the charge. For $n \geq 5$, significantly less charge is being dispersed upon addition of another H_2O. This signifies that charge dispersion is the major cause of clustering stabilization up to just 4 H_2O while normal hydrogen bonding is predominant thereafter. Previous studies of pure water clusters and hydrated electrons show that ΔG is positive for small clusters but becomes negative for clusters containing ca. 4 H_2O. Addition of further H_2O leads to increased stabilization which, similar to the present findings quickly converge to values close to those of hydrated water (Lee et al., 2005; Maheshwary et al., 2001). We thereby conclude that the strong stablization of the clusters, up to $n = 4$, is due to dispersion of the extra electron, while the moderate additional stabilization is due to normal hydrogen bonding as

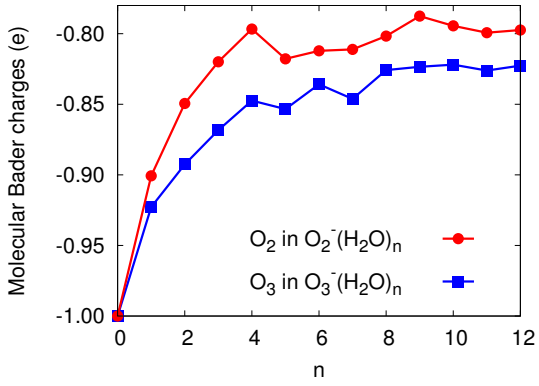

Fig. 6. Development of charge as function of number of water molecules. Both in the O_2^- and O_3^- clusters, an increasing amount of charge is delocalized up to $n = 4$ whereafter changes are moderate. At $n = 12$, the delocalization has converged and ca. 0.80 e and 0.82 e remains on the O_2 and O_3 species, respectively.

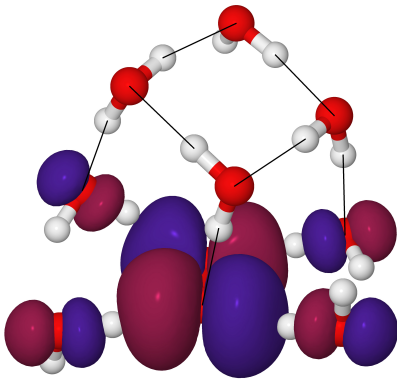

Fig. 7. Plot of HOMO orbital of the $O_2^-(H_2O)_8$ cluster. Hydrogen bonds are indicated by black lines. Electronic density cutoff is 0.02 e/a_0^3. The delocalization of the excess charge onto the 4 closest H_2O is apparent.

also found in pure water clusters and for the hydrated electron.

This is again apparent when investigating the HOMO orbital that facilitates the extra electron. As an example is the HOMO orbital of the $O_2^-(H_2O)_8$ system illustrated in Fig. 7. As is seen from the spatial distribution of the orbital, only the 4 closest H_2O molecules contribute significantly while the remaining H_2O are stabilized by a network of hydrogen bonds.

3.4 Tropospheric size distribution

It is well known that for several gas phase reactions, the degree of hydration may be important both for the kinetic and thermodynamic properties (Kurtén et al., 2007; Bandy and Ianni, 1998). Hence, it is of interest to study the distribution of the clusters at varying temperatures and pressures corresponding to typical tropospheric conditions (Mhin et al., 1993). Therefore, we have determined the mole fractions at varying altitudes, assuming a constant lapse rate of 6.5 °C, a ground level temperature of 15 °C and a constant relative humidity (RH) of 25 %. Further, thermal equilibrium is assumed and both sources and sinks are neglected. Thereby, the mole fractions of the various clusters readily can be deduced via Eq. (2). The results are shown in Fig. 8. For clarity, only the 5 most probable clusters are shown.

First, we note that the mole fractions are very sensitive to the amount of water vapor. In more humid atmospheres, the clusters readily grow while smaller clusters are more probable at drier conditions. However, under all conditions will clusters of multiple sizes co-exsist. Also apparent from Fig. 8, is that smaller clusters dominate at lower altitudes due to the higher temperatures favoring water evaporation. However, only under extremely dry conditions (RH <0.1 %) are the distributions dominated by clusters smaller than $n = 5$.

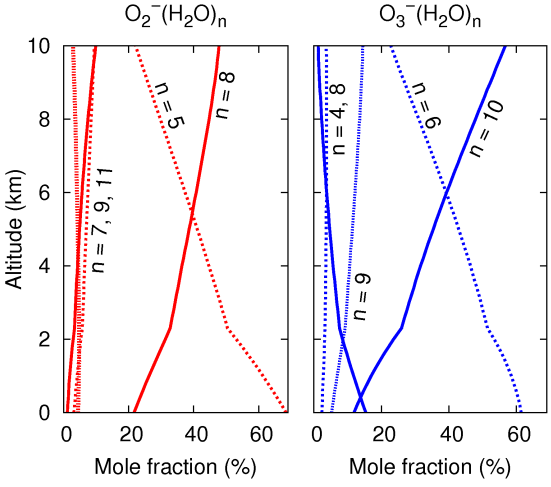

Fig. 8. Mole fraction as function of altitude. The distributions are very sensitive to the water vapor pressure - here shown for 25 % RH. For clarity only the 5 most populated structures are shown. At the altitude of freezing, ca. 2.3 km, the water vapor equilibrate with ice in stead of liquid water- hence the kinks.

Secondly, the distribution around the altitude of freezing is interesting, here found at ca. 2.3 km, whereafter gaseous H_2O must equilibrate with ice rather than liquid water. This effect delays the tendency of cluster growth at increasing altitudes due to decreasing temperatures, and is seen as a kink in Fig. 8.

3.5 Simple chemistry

One possible evolution of the $O_2^-(H_2O)_n$ and $O_3^-(H_2O)_n$ clusters is evaporation of neutral O_2 or O_3 resulting in a hydrated electron, i.e. the reaction

$$O_x^-(H_2O)_n \rightarrow O_x + (H_2O)_n^- . \quad \text{(R3)}$$

This can be evaluated as the sum of the reactions

$$O_x^-(H_2O)_n \rightarrow O_x^- + n\,H_2O \quad \text{(R4)}$$

$$O_x^- \rightarrow O_x + e^- \quad \text{(R5)}$$

$$n\,H_2O \rightarrow (H_2O)_n \quad \text{(R6)}$$

$$(H_2O)_n + e^- \rightarrow (H_2O)_n^-. \quad \text{(R7)}$$

The thermodynamics of Reactions (R4–R7) is given as the accumulated binding energies of Table 1, the electron affinity of O_x, the cohesive energy of neutral water clusters (Lee et al., 2005), and the adiabatic electron affinity of the water cluster (Lee et al., 2003, 2005), respectively. These values are tabulized in the Supplement. No in-depth discussion will be given, but it is thereby apparent that Reaction (R3) is at least 75 kJ/mol endothermic for O_2 evaporation and at least 210 kJ/mol endothermic for O_3 evaporation. Hence, it is clear that Reaction (R3) is without relevance for atmospheric chemistry.

We also note that previous studies of the vertical electronic detachment energies of these clusters show that this event is negligible under atmospheric conditions (Luong et al., 2001; Novakovskaya and Stepanov, 2004).

Of high relevance, however, is the charge transfer process between $O_2^-(H_2O)_n$ clusters and O_3. An electron produced by a cosmic ray impact will most likely attach to an O_2 molecule, due to the high atmospheric concentration of O_2. Since H_2O is much more abundant than O_3, the initial O_2^- ion will hydrate to equilibrium before colliding with an O_3 molecule.

From the electron affinities it is known that the charge transfer is ca. 160 kJ/mol exothermic for $n = 0$. From Figs. 1 and 2 it is however apparent that several of the $O_2^-(H_2O)_n$ clusters are significantly more stable than the corresponding $O_3^-(H_2O)_n$ clusters and that the charge transfer process will become correspondingly less exothermic. E.g. is the $O_2^-(H_2O)_1$ cluster 13 kJ/mol more stable towards dissociation than the $O_3^-(H_2O)_1$ cluster. Consequently is the charge transfer reaction

$$O_2^-(H_2O)_1 + O_3 \rightarrow O_2 + O_2^-(H_2O)_1 \quad (4)$$

only ca. 147 kJ/mol exothermic. However, evaluating the numbers yields that at no point is the reaction less than 100 kJ/mol exothermic and the Gibbs free energy converge to ca. −110 kJ/mol for large clusters. We thus conclude that transfer of an electron to an O_3 molecule from a $O_2^-(H_2O)_n$ cluster is a likely process for an atmospheric electron generated by a cosmic ray.

4 Conclusions

An ab initio study of $O_2^-(H_2O)_n$ and $O_3^-(H_2O)_n$ clusters is presented. We have determined the thermodynamics of cluster growth via stepwise addition of H_2O. The resulting structures show clear shell structure and filling up the first hydration shell, consisting of 5 H_2O, is highly exothermic. Filling up the second shell is significantly less exothermic, and weather or not it will be filled depends on both temperature and humidity.

The results are in good agreement with experimental data, available for clusters containing up to 3 H_2O (Arshadi and Kebarle, 1970; Fehsenfeld and Ferguson, 1974). Furthermore, the thermodynamics converges smoothly towards hydrated H_2O as required, and is thus confirmed for both small and large clusters. The smooth convergence is also in accordance with experiment (Yang and Castleman, 1990; Skalny et al., 2008).

In all systems, the central ion is located at or near the surface of the hydrogen bonded network and the excess electron is in all clusters at least 80 % localized at the O_2 or O_3 species. This signifies that the central ion retains much of its reactivity despite hydration and is easily accessible to further chemical reactions.

Finally, we assessed the reactivity of the clusters towards a few simple reactions. Detachment of an electron or evaporation of a neutral O_2 or O_3 was found negligible, but charge transfer from a $O_2^-(H_2O)_n$ cluster to an O_3 molecule is very exothermic, regardless of hydration level.

We conclude that these clusters are stable under atmospheric conditions, at least up to $n = 5$ and show no sign of chemical inactivation at increased hydration. These clusters thus remain of interest for ion induced atmospheric chemistry.

In order to investigate larger clusters and their impact on the scattering of electromagnetic radiation from the Sun and the Earth we will in future investigations utilize the methods presented by Poulsen et al. (2001, 2002) and Jensen et al. (2000).

Acknowledgements. The authors thank Nigel Calder for assistance in prepararing of this manuscript and the Danish Center for Scientific Computing for access to computing facilities. Further, T. K. thanks the Academy of Finland for funding and the CSC IT Centre for Science in Espoo, Finland for computer time and M. B. E. thanks the Carlsberg Foundation for financial support. K.V.M. thanks the Danish Natural Science Research Council/ The Danish Councils for Independent Research and the Villum Kann Rasmussen Foundation for financial support.

Edited by: A. Laaksonen

Supplement related to this article is available online at: http://www.atmos-chem-phys.net/11/7133/2011/acp-11-7133-2011-supplement.pdf.

References

Adler, T. B., Knizia, G., and Werner, H. J.: A simple and efficient CCSD (T)-F12 approximation, J. Chem. Phys., 127, 221106, doi:10.1063/1.2817618, 2007.

Arshadi, M. and Kebarle, P.: Hydration of $OH^-$and O_2^- in the gas phase. Comparative solvation of OH-by water and the hydrogen halides. Effects of acidity, J. Chem. Phys., 74, 1483–1485, 1970.

Bader, R. F. W.: Atoms in molecules: a quantum theory, Clarendon Press Oxford, USA, 458 pp., 1990.

Bader, R. F. W.: 1997 Polanyi Award Lecture Why are there atoms in chemistry?, Can. J. Chem., 76, 973–988, 1998.

Bandy, A. R. and Ianni, J. C.: Study of the hydrates of H_2SO_4 using density functional theory, J. Phys. Chem. A, 102, 6533–6539, 1998.

Bork, N., Bonanos, N., Rossmeisl, J., and Vegge, T.: Ab initio charge analysis of pure and hydrogenated perovskites, J. Appl. Phys., 109, 033702, doi:10.1063/1.3536484, 2011.

Carslaw, K., Harrison, R., and Kirkby, J.: Cosmic rays, clouds, and climate, Science, 298(5599), 1732–1737, doi:10.1126/science.1076964, 2002.

Cochran, W.: Effective Ionic Charge in Crystals, Nature, 191, 60–61 doi:10.1038/191060c0, 1961.

Corana, A., Marchesi, M., Martini, C., and Ridella, S.: Minimizing multimodal functions of continuous variables with the simulated annealing algorithm, ACM Transactions on Mathematical Software (TOMS), 13, 262–280, 1987.

Dunning, T. H. J.: Gaussian basis sets for use in correlated molecular calculations. I. The atoms boron through neon and hydrogen, J. Chem. Phys., 90(2), 1007–1023, 1989.

Enghoff, M. B. and Svensmark, H.: The role of atmospheric ions in aerosol nucleation- a review, Atmos. Chem. Phys., 8, 4911–4923, doi:10.5194/acp-8-4911-2008, 2008.

Enghoff, M. B., Pedersen, J. O. P., Bondo, T., Johnson, M. S., Paling, S., and Svensmark, H.: Evidence for the role of ions in aerosol nucleation, J. Phys. Chem. A, 112, 10305–10309, 2008.

Fehsenfeld, F. and Ferguson, E.: Laboratory studies of negative ion reactions with atmospheric trace constituents, J. Chem. Phys., 61(8), 3181–3193, doi:10.1063/1.1682474, 1974.

Gross, A., Nielsen, O. J., and Mikkelsen K. V.: From molecules to droplets, Adv. Quant. Chem. 55, 355–385, 2008.

Harrison, R. and Carslaw, K.: Ion-aerosol-cloud processes in the lower atmosphere, Rev. Geophys., 41(3), 1012, doi:10.1029/2002RG000114, 2003.

Henkelman, G., Arnaldsson, A., and Jónsson, H.: A fast and robust algorithm for Bader decomposition of charge density, Comp. Mat. Sci., 36, 354–360, 2006.

Hvelplund, P., Kadhane, U., Nielsen, S. B., Panja, S., and Støchkel, K.: On the formation of water-containing negatively charged clusters from atmospheric pressure corona discharge in air, Int. J. Mass Spectrom., 292, 48–52, 2010.

Jensen, F.: Describing anions by density functional theory: Fractional electron affinity, J. Chem. Theory Comput., 6, 2726–2735, 2010.

Jensen, L., Schmidt, O. H., Mikkelsen, K. V., Astrand, P.-O.: Static and frequency-dependent polarizability tensors for carbon nanotubes, J. Phys. Chem. B 104, 10462–10466, 2000.

Kurtén, T., Noppel, M., Vehkamäki, H., Salonen, M., and Kulmala, M.: Quantum chemical studies of hydrate formation of H_2SO_4 and HSO_4, Boreal Environ. Res., 12, 431–453, 2007.

Kurtén, T., Loukonen, V., Vehkamäki, H., and Kulmala, M.: Amines are likely to enhance neutral and ion-induced sulfuric acid-water nucleation in the atmosphere more effectively than ammonia, Atmos. Chem. Phys., 8, 4095–4103, doi:10.5194/acp-8-4095-2008, 2008.

Lee, H. M. and Kim, K. S.: Ab initio study of superoxide anionwater clusters $O_2^-(H_2O)_{n=1-5}$, Molec. Phys., 100, 875–879, 2002.

Lee, H. M., Lee, S., and Kim, K.: Structures, energetics, and spectra of electron-water clusters, $e^-(H_2O)_{2-6}$ and $e^-HOD(D_2O)_{1-5}$, J. Chem. Phys., 119, 187–194, doi:10.1063/1.1576757, 2003.

Lee, H. M., Suh, S. B., Tarakeshwar, P., and Kim, K. S.: Origin of the magic numbers of water clusters with an excess electron, J. Chem. Phys., 122, 044309, doi:10.1063/1.1834502, 2005.

Li, X., Millam, J. M., and Schlegel, H. B.: Ab initio molecular dynamics studies of the photodissociation of formaldehyde, HCO→ H + CO: Direct classical trajectory calculations by MP2 and density functional theory, J. Chem. Phys., 113, 10062, doi:10.1063/1.1323503, 2000.

Lide, D. R.: Handbook of Chemistry and Physics, CRC Press., 5–18, 1997.

Loboda, O. and Goncharuk, V.: Theoretical research into interaction of water clusters with ozone, J. Water Chem. Technol., 31, 213–219, 2009.

Luong, A., Clements, T., Resat, M. S., and Continetti, R.: Energetics and dissociative photodetachment dynamics of superoxide–water clusters: $O_2^-(H_2O)_n$, n= 1–6, J. Chem. Phys., 114, 3449–3455, doi:10.1063/1.1342221, 2001.

Maheshwary, S., Patel, N., Sathyamurthy, N., Kulkarni, A. D., and Gadre, S. R.: Structure and Stability of Water Clusters $(H_2O)_n$, $n = 8$–20: An Ab Initio Investigation, J. Phys. Chem. A, 105, 10525–10537, 2001.

Manby, F.: Density fitting in second-order linear-r12 Møller–Plesset perturbation theory, J. Chem. Phys, 119, 4607, doi:10.1063/1.1594713, 2003.

Marsh, N. D. and Svensmark, H.: Low cloud properties influenced by cosmic rays, Phys. Rev. Lett., 85, 5004–5007, 2000.

Mhin, B. J. Lee, S. J., and Kim, K.S.: Water-cluster distribution with respect to pressure and temperature in the gas phase, Phys. Rev. A, 48, 5, 3764–3770, 1993

Nadykto, A. B., Al Natsheh, A., Yu, F. Q., Mikkelsen, K. V., and Ruuskanen, J.: Quantum nature of the sign preference in ion-induced nucleation, Phys. Rev. Lett. 96, 125701, doi:10.1103/96.125701, 2006.

Nadykto, A. B., Al Natsheh, A., Yu, F. Q., Mikkelsen, K. V., and Herb, J.: Computational quantum chemistry: A new approach to atmospheric nucleation, Adv. Quant. Chem. 55, 449–478, 2008.

Novakovskaya, Y. V. and Stepanov, N. F.: Ultraviolet-light absorption and electron localization by ozone in the presence of water: nonempirical consideration, in: Proc. SPIE, 5311, p. 245, 2004.

Peach, M. J. G., Helgaker, T., Sałek, P., Keal, T. W., Lutnæs, O. B., Tozer, D. J., and Handy, N. C.: Assessment of a Coulomb-attenuated exchange-correlation energy functional, Phys. Chem. Chem. Phys., 8, 558–562, 2006.

Peterson, K. A., Adler, T. B., and Werner, H. J.: Systematically convergent basis sets for explicitly correlated wavefunctions: The atoms H, He, B–Ne, and Al–Ar, J. Chem. Phys., 128, 084102, doi:10.1063/1.2831537, 2008.

Poulsen, T. D., Kongsted, J., Osted, A., Ogilby, P. R., and Mikkelsen, K. V.: The combined multiconfigurational self-

consistent-field/molecular mechanics wave function approach, J. Chem. Phys. 115, 2393–2400, 2001.

Poulsen, T. D., Ogilby, P. R., and Mikkelsen, K. V.: Linear response properties for solvated molecules described by a combined multi-configurational self-consistent-field/molecular mechanics model, J. Chem. Phys. 116, 3730–3738, 2002.

Ryabinkin, I. and Novakovskaya, Y. V.: Nonempirical Description of the Atmospherically Important Anionic Species. II. Hydrated Ozone Anions, Struct. Chem., 15, 71–75, 2004.

Santos, M. V. P., Teixeira, E. S., and Longo, R. L.: A direct dynamics study of protonated alcohol dehydration and the Diels-Alder reaction, J. Brazil Chem. Soc., 20, 652–662, 2009.

Seta, T., Yamamoto, M., Nishioka, M., and Sadakata, M.: Structures of Hydrated Oxygen Anion Clusters: DFT Calculations for $O^-(H_2O)_n$, $O_2^-(H_2O)_n$, and $O_3^-(H_2O)_n$ ($n = 0$–4), J. Phys. Chem. A, 107, 962–967, 2003.

Skalny, J. D., Orszagh, J., Mason, N. J., Rees, J. A., Aranda-Gonzalvo, Y., and Whitmore, T. D.: Mass spectrometric study of negative ions extracted from point to plane negative corona discharge in ambient air at atmospheric pressure, Int. J. Mass Spectrom., 272, 12–21, 2008.

Svensmark, H., Bondo, T., and Svensmark, J.: Cosmic ray decreases affect atmospheric aerosols and clouds, Geophys. Res. Lett., 36, L15101, doi:10.1029/2009GL038429, 2009.

Tachikawa, H. and Abe, S.: Structures and excitation energies of ozone-water clusters $O_3(H_2O)_n$ (n= 1-4), Inorg. Chim. Acta, 358, 288–294, 2005.

Tang, W., Sanville, E., and Henkelman, G.: A grid-based Bader analysis algorithm without lattice bias, J. Phys. Condens. Matt., 21, 084204, doi:10.1088/0953-8984/21/8/084204, 2009.

Weber, J. M., Kelley, J. A., Nielsen, S. B., Ayotte, P., and Johnson, M. A.: Isolating the spectroscopic signature of a hydration shell with the use of clusters: Superoxide tetrahydrate, Science, 287(5462), 2461–2463, doi:10.1126/science.287.5462.2461, 2000.

Weigend, F.: A fully direct RI-HF algorithm: Implementation, optimised auxiliary basis sets, demonstration of accuracy and efficiency, Phys. Chem. Chem. Phys., 4, 4285–4291, 2002.

Weigend, F., Köhn, A., and Hättig, C.: Efficient use of the correlation consistent basis sets in resolution of the identity MP2 calculations, J. Chem. Phys., 116, 3175–3183, doi:10.1063/1.1445115, 2002.

Werner, H. J., Adler, T. B., and Manby, F. R.: General orbital invariant MP2-F12 theory, J. Chem. Phys., 126, 164102, doi:10.1063/1.2712434, 2007.

Yanai, T., Tew, D. P., and Handy, N. C.: A new hybrid exchange-correlation functional using the Coulomb-attenuating method (CAM-B3LYP), Chem. Phys. Lett., 393, 51–57, 2004.

Yang, X. and Castleman, A.: Production and magic numbers of large hydrated anion clusters $X^-(H_2O)_{N=0-59}$ (X = OH, O, O_2, O_3) under thermal conditions, J. Phys. Chem., 94, 8500–8502, 1990.

Yousaf, K. E. and Peterson, K. A.: Optimized auxiliary basis sets for explicitly correlated methods, J. Chem. Phys., 129, 184108, doi:10.1063/1.3009271, 2008.